Particle Accelerators, 1992, Vols. 37–38, pp. 361–370
Reprints available directly from the publisher
Photocopying permitted by license only

STOPPING OF ENERGETIC SULFUR AND BROMINE IONS IN DENSE HYDROGEN PLASMA

D. GARDÈS, R. BIMBOT, M. F. RIVET, A. SERVAJEAN
(IPN, CNRS: Groupe de Recherche 918, Orsay, France)

C. FLEURIER, D. HONG
(GREMI, Orléans, France)

C. DEUTSCH and G. MAYNARD
(LPGP, Orsay, France)

(Received 3 December 1990)

The stopping power of sulfur and bromine ions traversing a fully ionized hydrogen plasma has been determined by coupling a plasma target to the heavy ion beam of the Orsay Tandem accelerator. Measured energy losses are well reproduced by the Standard Stopping Model and they clearly demonstrated the enhanced stopping power of a plasma (free electrons) relative to cold matter (bound electrons). The determination of mean effective charge state during the stopping process is discussed in relation to theoretical predictions.

1 INTRODUCTION

Beam-plasma interaction experiments allow one to investigate a new domain of the ion-matter interactions that is of fundamental interest for atomic physics and plasma physics. Beyond the interest of fundamental investigations, the knowledge of the energy deposition of intense beams in ionized matter is essential with respect to heavy ion inertial confinement fusion (ICF) studies. In both cases of direct or indirect drive for ICF scenario, the first step of the energy deposition on the ICF pellet corresponds to a transfer of the kinetic energy of the incident beam in collective modes, generating compression and heating of the pellet surface, and the stopping process takes place in a corona plasma resulting from the rapid ablation of the target surface. Precise knowledge of the energy deposition process is of prime importance in order to determine the thickness of the target tamper.

There has been many theoretical approaches of this problem, but only a few experimental data were available to confirm these theories. The experimental program described here presents a complete set of stopping power measurements obtained during the last four years in a joint collaboration between French and German laboratories.

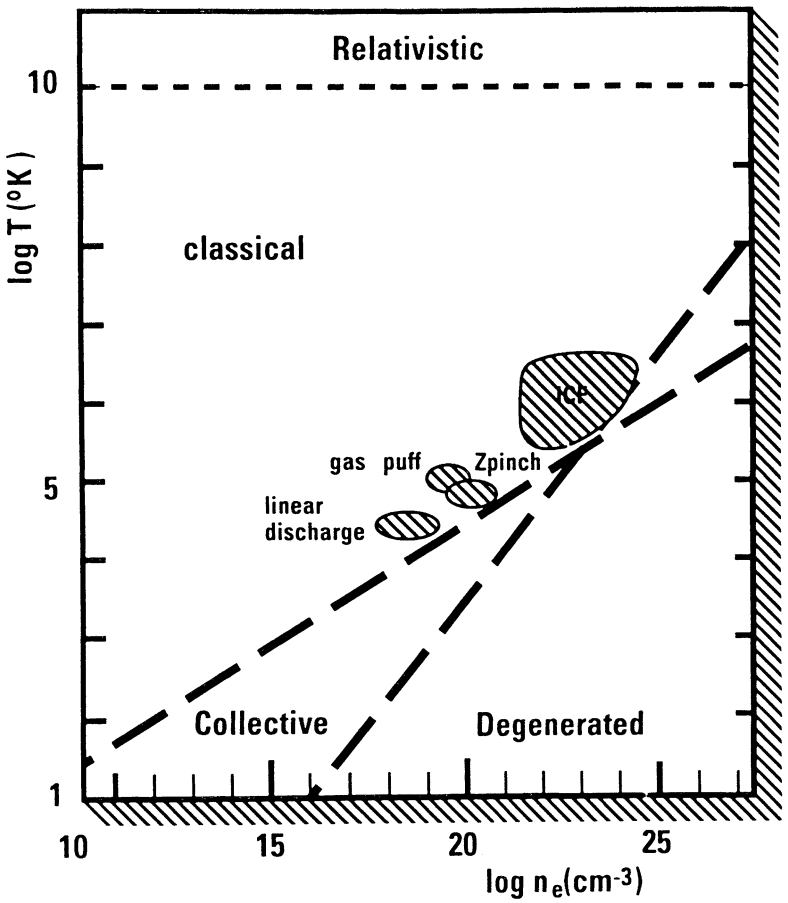

FIGURE 1 Temperature-density diagram for the plasmas in this study.

The basic idea was to couple an external plasma target to an accelerator beam line and let the heavy ions flow through the plasma. This simulation of the interaction between an intense ion beam and the ablation plasma is only valid because of the so-called reduction principle[1] which stipulates that even with intense beams, the average ion-ion distance within the beam remains two order of magnitude larger than the electron Debye screening length. This effect suppresses largely collective effects in the entrance channel, and allows one to treat the interaction as a simple ion-electron or ion-ion collision.

Figure 1 shows the characteristics of the plasma target that have been involved in these experiments.

In this temperature-density diagram, are reported experimental plasmas compared to the ablation-compression plasma related to the ICF process. All these plasmas are supposed to be relevant of typical classical, non-degenerated plasmas.

This paper is mainly devoted to interactions with a hydrogen plasma produced in

linear discharge, which have been extensively studied during the first step of this program.[2–4]

2 THEORETICAL BACKGROUND

Swift heavy ions penetrating into a plasma column interact mainly with free electrons, inducing inelastic processes. The energy transfer is much more efficient than the corresponding interaction with bound electrons. Two reasons explain such a behavior:

- Free electron orbitals show the most efficient stopping due to their flexibility to respond to the incoming electrostatic field.
- The effective charge of the incident ion is rapidly increased up to the equilibrium charge and recombination mechanisms are strongly inhibited.

The framework of the stopping standard model (SSM) consists of a generalization of the well-known Bethe-Bohr-Bloch theory, extended to ion-plasma interaction. Based on a few assumptions[5] this model predicts a stopping power enhanced by about a factor of two relative to the same conditions of electron density in cold matter.

When the projectile velocity exceeds the thermal velocity of the free electrons in the plasma (high-velocity approximation), the general expression of the stopping power takes the form

$$-(dE/dx) = 4\cdot(Z^*e^2)^2 n_t/V_i^2 \cdot L(V_i, Z^*)$$

where Z^* is the mean ionization state of the ion during the stopping process, n_t is the plasma density, and V_i is the ion velocity. The stopping number $L(V_i, Z^*)$ includes bound and free electron contributions $L = L_0^B + L_0^F$ (atomic units):

$$L_0^B = \text{Log}\, 2V_i^2/I$$

where I is the mean ionisation potential energy for hydrogen, and

$$L_0^F = \text{Log}\, 2V_i^2/w_p,$$

where w_p is the plasma frequency. As long as $w_p \ll I$, the free electron contribution is dominant in the stopping process.

Beyond the more efficient energy exchange due to free electrons, the enhanced projectile effective charge amplifies this effect. Numerical simulation of the charge-state evolution during interaction with free electrons of a plasma predicts that the balance between ionisation processes and bound-bound, radiative and dielectronic recombinations leads to an intense stripping of the incident ion due to the relatively low cross sections of the recombination processes. For the 10^{17} e^-/cm^3 plasma in these experiments, we thus expect to observe a rapid increase of the effective charge at the entrance of the plasma target; then the charge remains unchanged during the stopping process, except at the end of the trajectory when the velocity of the ion decreases rapidly.

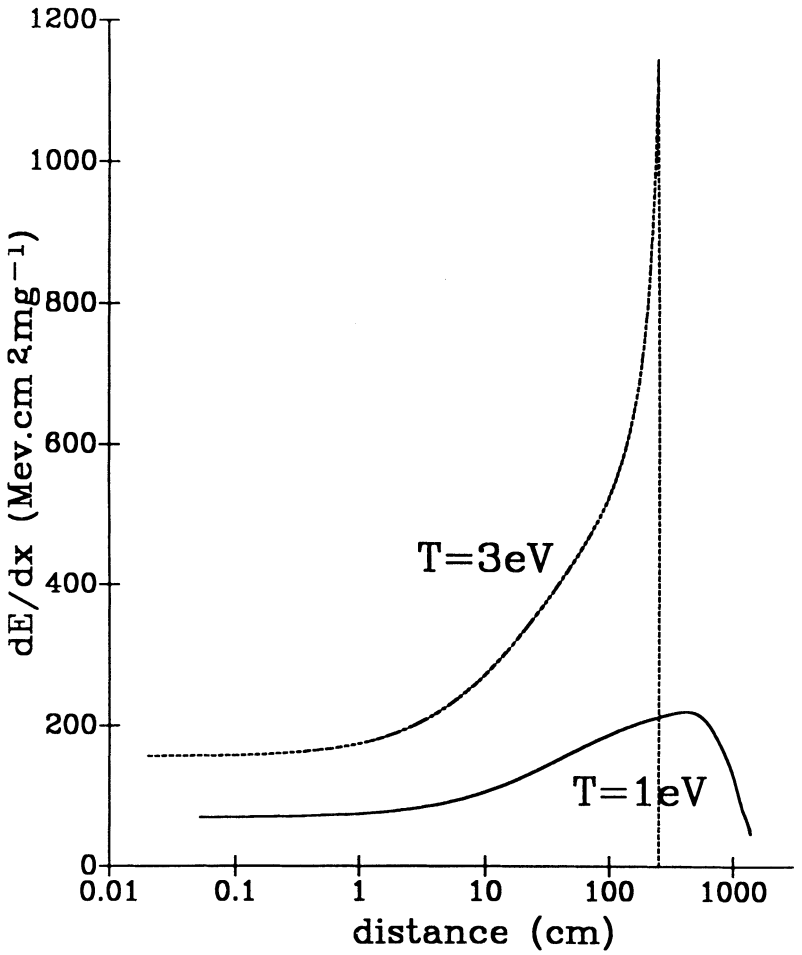

FIGURE 2 Calculated stopping power dE/dx for a Br ion in H plasma (3 eV line) of a cold H_2 gas target (1 eV line).

The addition of these two effects (efficiency of free electron stopping and enhanced ionization of the projectile), results in a range-shortening of heavy ions in the plasma compared to the same density of cold-gas bound electrons. Figure 2 presents the calculated stopping power dE/dX for a bromine ion penetrating a cold hydrogen gas target (1 eV line) or the corresponding plasma target (density 2×10^{17} e^-/cm^3; 3 eV line).

In the case of a plasma target, the Bragg curve exhibits a pronounced maximum at the end of the trajectory, allowing an intense and localized energy deposition. Such a behavior is particularly favorable in the perspective of energy deposition in an ICF pellet, where we expect to deposit the projectile energy in a narrow range in order to avoid preheating of the target core.

3 BEAM-PLASMA INTERACTION EXPERIMENTS

3.1 Experimental Set-up

The basic feature of the experimental set-up is coupling of a hydrogen plasma column with the beam line of a heavy ion accelerator. Two similar devices have been used simultaneously at Orsay in France and at Darmstadt in Germany, in order to investigate beam-plasma interactions over a wide range of incident ions (from carbon up to uranium) and velocities.

A specific effort has been made on the design of the following elements:

- Plasma diagnostics.
- Coupling ports between plasma target and the beam line.
- Time of flight measurements and acquisition process.

3.1.1 Plasma Target A steady flow of hydrogen gas (5–10 mbar) is established inside a quartz cylinder (5 cm diameter, 40 cm length). The complete ionization of hydrogen gas is achieved by ohmic heating using a powerful electric discharge yielding a total energy of 5 kJ when operated at 15 kV.

The maximum ionization of the hydrogen plasma occurred 10 to 20 μs after ignition, depending on the intensity of the electrical discharge. The magnetic field produced by the current flowing through the plasma tends to constrict the plasma column (Z-pinch effect). This effect is partially inhibited in our case by the thermal pressure of the plasma. This magnetic confinement prevents direct contact with the walls of the plasma tube and improves the stability and purity of the plasma during about 60 μs. In return, this magnetic field structure induces deflection forces on the ion beam. As a result we observe a succession of focusing and defocusing configurations in the plasma tube which alter or on the contrary improve the transmission of the beam through the plasma column. These plasma lens effects have been discussed in previous papers[2] and we are paying great attention to the focusing properties of the linear Z pinch in prospect of future applications; the properties of the Z-pinch column are already investigated for achieving the final focusing of intense bunches of the SIS-ESR beams.[6]

3.1.2 Coupling Ports The typical plasma lifetime is approximately 100 μs. Therefore the plasma tube needs only to be open on the beam line during this short time. Special coupling ports located at both sides of the plasma tube were therefore developed,[9] namely two fast valves which can be retracted within 200 μs (total aperture). This limits the hydrogen leakage during the measurement. During the ignition of the plasma column there always remains a few centimeters of molecular hydrogen at both ends of the plasma tube. This "cold" hydrogen is of great importance for the exact estimation of the projectile charge state at the entrance of the plasma. Thus, a crucial improvement related to this shutter device is the reduction of cold gas layers at both extremities of the plasma target[7]. This system allows one to use more expensive gases such as deuterium, which have properties that stabilize the discharge and improve the reproducibility from shot to shot.

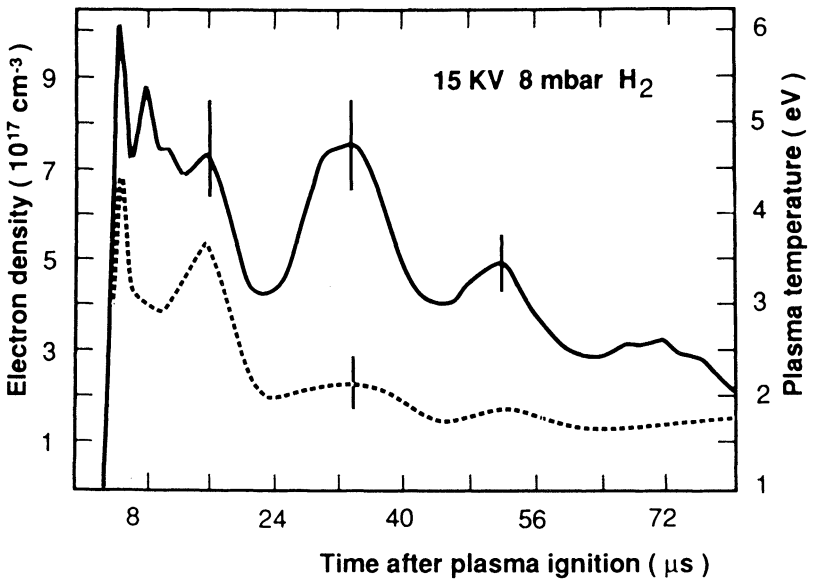

FIGURE 3 Time evolution of free electron density and plasma pressure.

3.1.3 Plasma Diagnostic Plasma diagnostics were performed using three optical methods[8]. The free-electron density and temperature were determined from:

- Emission spectroscopy using Stark-broadening of the hydrogenic H_β line.
- Simultaneous absorption measurement at two different laser wavelengths (Ar laser).
- Laser interferometry. The optical length depends on the refraction index of the plasma which is fully determined by the electron density. (He–Ne laser).

Figure 3 reports the measured evolutions of free electron density (solid line) and plasma temperature (dashed line) as a function of time. A good agreement is obtained for the density determination using the three methods. The accuracy on the density measurement is on the order of 15%.

The oscillatory behavior of these curves is due to the oscillating current in the discharge circuit. At the end of the plasma shot a progressive contamination by silicon ions pulled out from the quartz walls lowers the temperature and consequently induces a rapid recombination of the free electrons. This particular problem has been solved recently by replacing the quartz tube by an alumina one. In this latter case the temperature remains constant during the complete measurement.

3.1.4 Data Acquisition The energy losses of the heavy ions were measured with a time of flight (TOF) technique using each beam burst as an energy probe. The accelerator pulsation was fixed at 2.5 MHz, which corresponds to one beam burst every 800 ns. During one plasma shot we were thus able to perform about 100 energy-loss samplings.

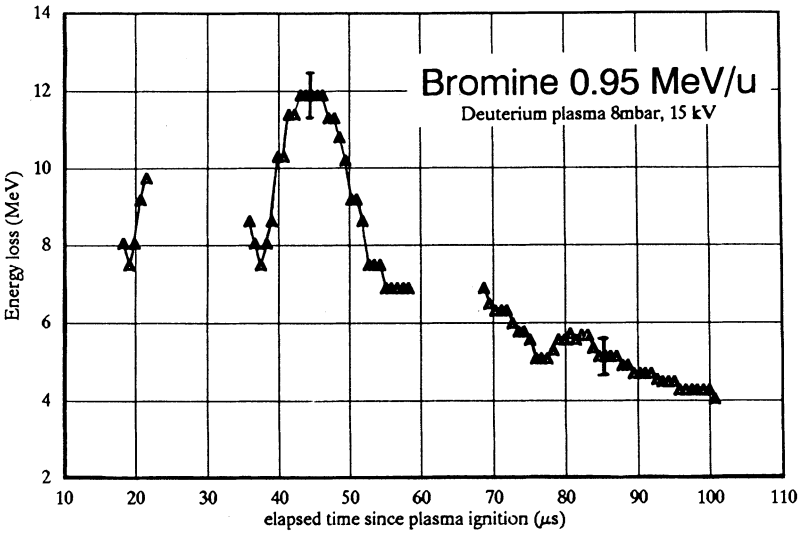

FIGURE 4 Energy loss measurements for a Br beam traversing a deuterium plasma target.

The plasma light emission was used to define the time zero of the acquisition process. The first beam bunch arriving after this light signal triggered the acquisition. Five capacitive phase probes placed at regular intervals along the beam line provided the timing signals. These signals were sent to a special time-to-digital-converter (TDC Multistops), which registered 255 stops following one start pulse. The time resolution of this device was 1 ns (0.05% of the full TOF) and its contribution to the global precision of the velocity measurement was thus negligible.

Several personal computers were devoted to the visualisation and memory storage of the data. Plasma parameters were registered simultaneously during each plasma shot.

3.2. Energy Loss Measurements

Energy loss measurements obtained with a bromine beam traversing a deuterium plasma target are presented in Figure 4.

The measured energy losses reproduce the oscillations of the plasma density and the error bars reflect the fluctuations between different plasma shots, demonstrating the good reproducibility of the plasma parameters.

The corresponding density curve indicates that in this particular measurement we have explored plasmas with densities evolving from $2.10^{17}\,e^-/cm^3$ up to $7.10^{17}\,e^-/cm^3$. By coupling energy losses measurements to their corresponding densities we are able to construct the curves, which are reported in Figure 5 for different incident ions.

All these have been obtained for incident ions covering a velocity range from 1 to

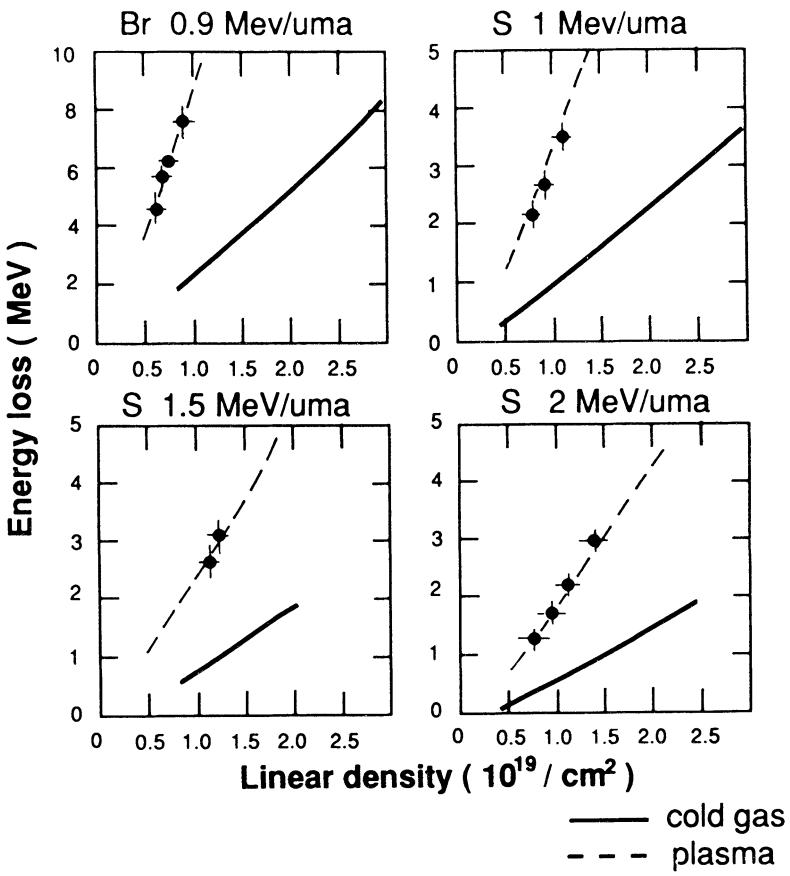

FIGURE 5 Energy loss as a function of linear plasma density for several incident ions. Solid lines refer to cold gas calculation; dashed lines correspond to SSM Theory.

2 cm/ns. This velocity region corresponds to the largest electronic stopping power for the considered ions.

Solid lines correspond to energy loss calculated values as a function of plasma density using the SSM theory. There is a fair agreement between experimental points and calculated values. This indicates that both estimations of projectile effective charge and stopping number evaluation are correctly taken into account.

3.3. Experimental Effective Charge State Determination.

If we consider two ions with the same velocity penetrating in the same plasma target, the only factor which differentiate their stopping powers is the square of their effective charge.

Measuring the energy loss allows charge-state determination, provided that we know a reference ion charge evolution. The carbon is a good candidate to be the reference ion. Due to its low atomic number, this ion reaches rapidly an equilibrium

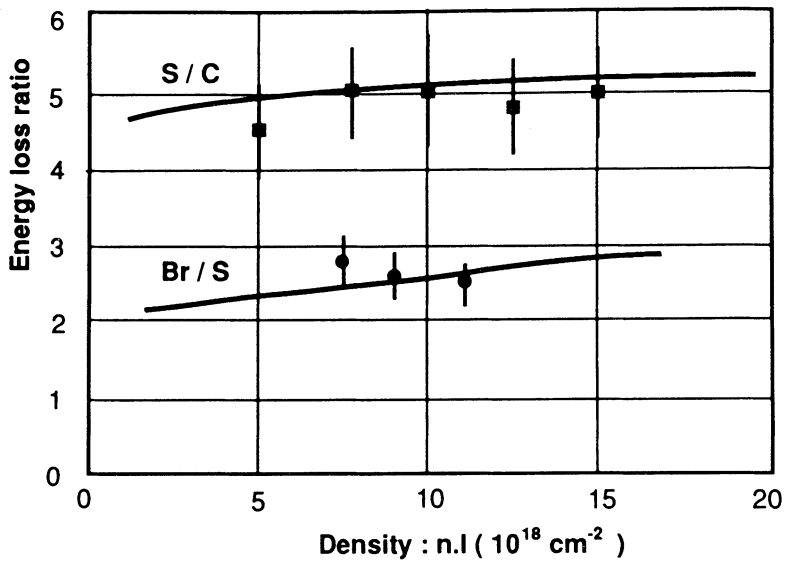

FIGURE 6 Energy loss as a function of effective charge.

charge very close to that of the fully ionised ion ($Z_{eff} = 5.95$). A comparison with the effective charge state evolution of the sulfur ion is presented in Figure 6. For each value of plasma density (or distance in hydrogen plasma) we can calculate the ratio of the square of the effective charge for the two ions. The corresponding curve is reported as a solid line on Figure 6.

The experimental determination of the ratio of the energy losses for the same ions traversing the same plasma densities are displayed as black points on the figure. The agreement is quite good and an extension of this mean charge determination is shown on the same diagram for the ion couple Br/S.

This method only gives access to mean values of the effective charge states and the natural development of this study will be a more refined analysis including a discrete charge state determination based on a magnetic analysis of the beam burst after interaction.

4 CONCLUSION AND FUTURE

This first step in the experimental approach of beam-plasma interactions has given a strong support for the validity of the SSM theory applied to hot matter. A wide range of heavy-ion species interacting with fully ionized hydrogen and deuterium plasmas was explored, and it was clearly demonstrated that the stopping power is enhanced, due to free electrons, in agreement with theoretical expectations.

The future of this experimental program is now to extend investigations in several directions:

• A progressive increase of the plasma densities and temperatures by varying plasma sources (Energetic Z pinch, gas puff generator, impact plasma from energetic and intense beam).

• A charge analysis of projectile ions after plasma interaction and the correlation with stopping power measurements.

• A more refined analysis of stopping process by varying the ionization ratio of the plasma target (by changing the gas support or the temperature)

REFERENCES

1. C. Deutsch, *Ann. Phys. (Paris)* **11** (1986) 1–111.
2. D. Gardès, R. Bimbot, S. Della Negra, M. Dumail, B. Kubica, A. Richard, M. F. Rivet, A. Servajean, C. Fleurier, A. Sanba, C. Deutsch, G. Maynard, D. H. H. Hoffmann, K. Weyrich and H. Wahl, *Europhys. Lett.* **8** (1988) 7 701–705.
3. D. Gardès, R. Bimbot, M. Dumail, B. Kubica, A. Richard, M. F. Rivet, A. Servajean, C. Fleurier, A. Sanba, D. Hong, C. Deutsch, G. Maynard, D. H. H. Hoffmann, K. Weyrich, and K. G. Dietrich *Rad. Effects and Defects in Solids* **110** (1989) 49–53.
4. D. H. H. Hoffmann, K. Weyrich, H. Wahl, R. Bimbot, D. Gardès, and C. Fleurier *Phys. Rev. A* **42**, 4 (1990) 2313–2321.
5. C. Deutsch, G. Maynard, R. Bimbot, D. Gardès, S. Della Negra, M. Dumail, B. Kubica, A. Richard, M. F. Rivet, A. Servajean, C. Fleurier, A. Sanba, D. H. H. Hoffmann, K. Weyrich, and H. Wahl, *Nucl. Instrum. Meth. A* **278** (1989) 38–43.
6. E. Boggasch, these *Proceedings; Proceedings of the Workshop on Plasma Focusing and Plasma Lenses*, (Darmstadt, Germany; January 1990).
7. D. Gardès, R. Bimbot, M. F. Rivet, A. Servajean, A. Fleurier, D. Hong, C. Deutsch, and G. Maynard, *Laser and Particle Beams* **8**, 4 (1990) 575–581.
8. C. Fleurier, A. Sanba, D. Hong, J. Mathias, J. C. Pellicer, *J. Phys. C* **7**, 49 (1988) 141–149.
9. C. Fleurier, J. Mathias, B. Dumax, J. Pellicer, A. Bonnet, D. Gardès, B. Kubica *Nucl. Instrum. Meth.* **B61** (1991) 236–238.